29th Congress of the International Council of the Aeronautical Sciences
St. Petersburg, Russia; September 7-12, 2014

FLIGHT DYNAMICS OF HIGHLY FLEXIBLE SOLAR-POWERED UAV BASED ON GEOMETRICALLY NONLINEAR INTRINSIC BEAM

Wang Rui *, Zhou Zhou *, Zhu Xiaoping **, Xu Xiaoping *
*** Science and Technology on UAV Laboratory, Northwestern Polytechnical University, Xi'an 710072, China,**
**** Institute of UAV, Northwestern Polytechnical University, Xi'an 710072, China**

Abstract

In order to obtain a convenient and precise method for the flight dynamics analysis of highly flexible solar-powered UAV, a geometrically nonlinear intrinsic beam model is introduced, it is employed to trim the UAV, and it is the base of the linearization of the flight dynamics and structure dynamics equations of motion. Proposed aerodynamics model is based on the Theodorsen unsteady aerodynamics model, it provides the Aerodynamics derivatives in every wing sections, their accumulation along the wing result in the derivatives of total UAV, and the aerodyanmics moment can be derived also by the applied arm of force. lifting-line theory is applied to accomplish the 3D aerodynamics effect correction. Base on these modeling and linearization efforts, four models are selected for comparison. The results show that, geometrically nonlinear equation of motion with 3D aeroelastics model is the only one which is able to accurately estimate the trimming and longitudinal flight dynamics behaviors, and the deformed model is quite accurate for lat-dir flight dynamics analysis.

Nomenclature

P	Linear momentum
H	Angular momentum
M	Mass, or moment
I	Moment of inertia
V	Linear velocity
Ω	Angular velocity
γ	Strain
κ	Curvature
f	External force
m	External moment
c	Chord
l	Wing span
C_{ab}	Direction cosine matrix from b to a
α	Angle of attack
β	Angle of side slip
x,y,z	Distance from the original at x,y,z directions

Subscript and superscript

g	Ground axis frame
R	Deformed beam axis frame at wing root
B	Deformed beam axis frame
b	Undeformed beam axis frame
M	Mean axis frame
s	Structure axis frame
a_B	Aero axis frame at Deformed beam
a_R	Aero axis frame at wing root
a_M	Aero axis frame at mean axis frame
$\{x\}_y$	Vector x expressed in y-frame
$\{x\}_{y,z}$	Z part of Vector x expressed in y-frame
x'	Spatial derivative of variable x
$\dot{x}$	Temporal derivative of variable x
$\bar{x}$	Mean value over the beam element
$\hat{x}$	Nodal value

1 Introduction

In preliminary design phase, the traditional flight dynamics analysis method is based on rigid flight dynamics model. The wing of high aspect-ratio solar-powered UAV is highly flexible, leading to significant geometrically nonlinear aeroelastic deformation during flight, and coupling between aeroelasticity and flight dynamics. If these have not been considered sufficiently, large error will occur. Even when analyzing the flight dynamics of highly flexible solar-powered UAV in conceptual design phase, the influence of aeroelastics must be considered. Therefore, a convenient and precise method should be established.

For the aeroelastic flight dynamics analysis of such a UAV, most papers ignored the aerodynamics force distribution characteristic along the span, and assumed the center of gravity (CG), elastic center (EC) and aerodynamics center (AC) to be coincide for simplification, and without considering the aerodynamics derivatives especially for the lateral-directional. In this paper, a more practical UAV model is proposed, in which the AC and EC is separated, the 3D quasi-steady aerodynamics force is considered, and aerodynamics derivatives in every wing sections are derived for accuracy.

The UAV discussed in this paper is equipped with 8 propulsion system nacelles (including secondary batteries, electrical motor and propeller and so on) and 5 vertical tails with the span of 70m and mean aerodynamics chord of 2.44m, which is shown in Fig.1.

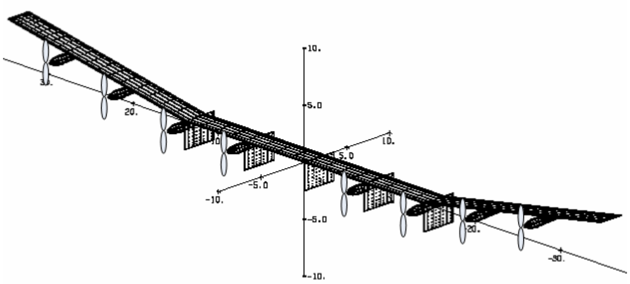

Fig.1 High aspect-ratio highly flexible solar-powered UAV

In this paper, in order to get a more accurate characteristic of solar-powered UAV, the mass parameters derived from conceptual design are employed, shown in Table 1, and the 3D effect of aerodynamics is considered.

Table 1 The mass parameters of high aspect-ratio solar-powered UAV

	Coefficient of mass	CG (from leading edge)	Elastic center
Structure	0.3	35%	35%
Solar array	0.15	45%	/
Propulsion system	0.5	0%	/
Payload	0.05	(at the CG of UAV)	/

This paper is organized as follows. Section 2 explains structural dynamics modeling based on the intrinsic beam Eq. [1, 2]. Section 3 introduces the models of force and moment applied to the UAV. Section 4 introduces the linearized model, including the longitudinal and lat-dir dynamics models, flight dynamics and structure dynamics models. Section 5 introduces the differences of trimming of 4 types of models. In section 5, the longitudinal and lat-dir modal of the flight dynamics is analyzed. Conclusion remarks are in section 7.

2 Structural Dynamic Modeling

The geometrically nonlinear structure flight dynamics equations are based on the intrinsic Beam equation derived by Hodges et al. shown as follows[1,2]:

$$
\begin{aligned}
&\dot{\bar P} + \tilde{\bar\Omega}\bar P = \bar F' + \tilde{\bar K}\bar F + \bar f \\
&\dot{\bar H} + \tilde{\bar\Omega}\bar H + \tilde{\bar V}\bar P = \bar M' + \tilde{\bar K}\bar M + (\tilde e_2 + \tilde{\bar\gamma})\bar F + \bar m \\
&\dot{\bar\gamma} = \bar V' + \tilde{\bar K}\bar V + (\tilde e_2 + \tilde{\bar\gamma})\bar\Omega \\
&\dot{\bar\kappa} = \bar\Omega' + \tilde{\bar K}\bar\Omega \\
&\dot{\hat P} + \tilde{\hat\Omega}\hat P = \hat f \\
&\dot{\hat H} + \tilde{\hat\Omega}\hat H = \hat m
\end{aligned}
\tag{1}
$$

The equations above are the core of structure dynamics, but they still can not be used for the analysis of aerodynamics and flight dynamics without the relationship of displacements and rotations. Hence, the kinematics motion must be established to obtain the relationship between strain and displacement. The position vector of the origin of the deformed beam frame (B-) in the root frame (R-) and their rotational relationship are [3]:

$$
\begin{aligned}
&\{r_B\}_R = C_{RB}(\gamma + e_2) \\
&C_{BR}{}' = -(\tilde\kappa + \tilde k)C_{BR}
\end{aligned}
\tag{2}
$$

The spatial derivatives can be replaced by the following equations, named central difference method[4]:

$$
\begin{aligned}
&x_i' = \frac{1}{2h}(x_{i+1} - x_{i-1}) \\
&x_i'' = \frac{1}{h^2}(x_{i+1} - 2x_i + x_{i-1}) \\
&x_i''' = \frac{1}{2h^3}(x_{i+2} - 2x_{i+1} + 2x_{i-1} - x_{i-2}) \\
&x_i'''' = \frac{1}{h^4}(x_{i+2} - 4x_{i+1} + 6x_i - 4x_{i-1} + x_{i-2})
\end{aligned}
\tag{3}
$$

Where, h is the distance between two points.

The mean axis is applied to simplify and linearize the equation of motion. In the mean axis(M-) frame, the linear and angular momentums due to elastic deformation are zero at every instantaneous, which eliminates the coupling between the rigid body modes and the structural mode and results in a reduced-order system with only six degrees-of-freedom.

Since the equations in Eq. (1) are written in the B-frame, the equations of motion of rigid mode can be derived by pre-multiplying all terms by C_{MB} to obtain components in the M-frame and integrating in it along the beam axis as follows[5]:

$$M_{tot}(\{\dot{V}_{cg}\}_M + \{\Omega_M\}_M \times \{V_{cg}\}_M) = \sum C_{MB_i}\{f_n\}_{B_i} \tag{4}$$

$$\begin{aligned}&\{I_{cg}\}_M\{\dot{\Omega}_M\}_M + \{\dot{I}_{cg}\}_M\{\Omega_M\}_M + \{\Omega_M\}_M \times (\{I_{cg}\}_M\{\Omega_M\}_M) \\ &= \sum\{r\}_M \times C_{MB_i}\{f_n\}_{B_i} + \sum C_{MB_i}\{m_i\}_{B_i} \\ &-\sum C_{MB_n}\{I_i\}_B\{\dot{\Omega}_i\}_B - \sum \dot{C}_{MB_n}\{I_i\}_B\{\Omega_i\}_B\end{aligned} \tag{5}$$

where, the linear and angular velocities are defined as:

$$\begin{aligned}\{V_{cg}\}_M &= \frac{1}{M_{tot}}\sum \mu_i C_{MB_i}V_i \\ \{\Omega_M\}_M &= \{I_{cg}\}_M^{-1}\sum\{r_{B_iM}\}_M \times \mu_i C_{MB_i}V_i\end{aligned} \tag{6}$$

The relationship of coordinate transformation is:

$$C_{MB} = C_{Mg}C_{gB} \tag{7}$$

The total moment of inertia of the UAV is solved as follow:

$$\{I_{cg}\}_M = \sum[C_{MB_i}I_iC_{MB_i}^T + (r_i^T r_i E - r_i r_i^T)m_i] \tag{8}$$

If the relative position of the rigid body does not vary significantly, $\{\dot{I}_{cg}\}_M$ can be approximated to be zero. If the motion of the UAV is limited to longitudinal only, the last two terms at the right hand of Eq. (5) also can equal to zero.

3 Force and Moment Modeling

3.1 Internal forces and moments model

The wing of solar-powered UAV may undergo large deformations during normal flight, while the strain is small, exhibiting geometrically nonlinear behaviors. Therefore, the small-strain assumption is suitable for this problem. The internal forces and moments are linearly related to the strains and curvatures, shown in Eq. (9)[6]:

$$\begin{bmatrix} F \\ M \end{bmatrix} = \begin{bmatrix} R & S \\ S^T & T \end{bmatrix}^{-1} \begin{bmatrix} \gamma \\ \kappa \end{bmatrix} \tag{9}$$

The wing is assumed to be a prismatic and isotropic beam with the shear center and tension axis coincident with the reference axis, by which the above equation can be derived as follows:

$$\begin{aligned}\begin{bmatrix} F_x \\ F_y \\ F_z \end{bmatrix} &= \begin{bmatrix} GA_x & & \\ & EA & \\ & & GA_z \end{bmatrix}\begin{bmatrix} \gamma_x \\ \gamma_y \\ \gamma_z \end{bmatrix} \\ \begin{bmatrix} M_x \\ M_y \\ M_z \end{bmatrix} &= \begin{bmatrix} EI_x & & \\ & GJ & \\ & & EI_z \end{bmatrix}\begin{bmatrix} \kappa_x \\ \kappa_y \\ \kappa_z \end{bmatrix}\end{aligned} \tag{10}$$

where, G represents the shear modulus; E represents Young's modulus; J represents the torsional constant; I_x and I_z represent the area moment of inertia along the x and z direction.

3.2 Aerodynamics model

In order to analyze the motion of the flexible UAV exactly, the aerodynamic force of vibrating-wings should be analyzed. In this paper, the Theodorsen unsteady aerodynamics model is adopted, which has been used widely for airfoil or large aspect ratio wings.

For the Theodorsen model, the wing section is described in figure 2:

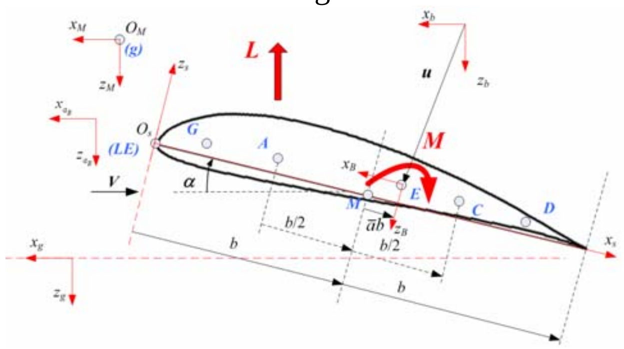

Fig.2 Illustration of wing section, coordinate systems and variables

where, the definition of points are:

LE: Leading Edge
G: center of Gravity of the wing section
g: center of Gravity of the UAV
A: Aerodynamics center
M: Middle point of chord

E: Elastic center, the position in x direction of s-frame is $\bar{a}b$

C: Control point of unsteady aerodynamics

D: Aerodynamics center of control surface

The definition of variables are:

α : angle of attack

b: length of 1/2 chord

u: deformation defined in B-frame

s-frame: the origin is at LE, x along the chord and pointing to the trailing edge, z perpendicular to x and point up

The formulation of Theodorsen unsteady aerodynamics force and its moment to the elastic center are:

$$
\begin{aligned}
C_L &= \pi b\left(\frac{\dot{\alpha}}{V}+\frac{\ddot{h}}{V^2}-\frac{b\bar{a}\ddot{\alpha}}{V^2}\right)+2\pi C(k)\left(\frac{\dot{h}}{V}+\alpha+b(\frac{1}{2}-\bar{a})\frac{\dot{\alpha}}{V}\right)\\
C_{M,E} &= \frac{\pi}{2}\left(\frac{b\bar{a}\ddot{h}}{V^2}-\frac{b^2}{V^2}(\frac{1}{8}+\bar{a}^2)\ddot{\alpha}-(\frac{1}{2}-\bar{a})\frac{b\dot{\alpha}}{V}\right)\\
&+\pi(\bar{a}+\frac{1}{2})C(k)\left(\frac{\dot{h}}{V}+\alpha+b(\frac{1}{2}-\bar{a})\frac{\dot{\alpha}}{V}\right)\\
&= \pi b\left(\frac{\dot{\alpha}}{V}[-(\frac{1}{4}-\frac{1}{2}\bar{a})]+\frac{\ddot{h}}{V^2}[\frac{1}{2}\bar{a}]-\frac{b\bar{a}\ddot{\alpha}}{V^2}[(\frac{1}{8}+\bar{a}^2)\frac{1}{2}b]\right)\\
&+[(\frac{1}{4}+\frac{1}{2}\bar{a})]2\pi C(k)\left(\frac{\dot{h}}{V}+\alpha+b(\frac{1}{2}-\bar{a})\frac{\dot{\alpha}}{V}\right)
\end{aligned}
\tag{11}
$$

where, 2π is the theoretic lift slope of airfoil; the steady aerodynamics center is at 1/4 chord; unsteady aerodynamics center and its control point is at 3/4 chord; all these variables can be replaced by the actual airfoil data. $C(k)$ is the Theodorsen function, produced by circulation. $k=\omega b/V$ is the reduced frequency. If k is low enough and $C(k)$ =0, the flow will become quasi-steady. As the flight dynamics of solar-powered UAV in low frequency is more concerned, quasi-steady flow assumption is adopt for analysis in this paper.

By applying the quasi-steady flow assumption and ignoring the terms in high orders, Eq.(11) becomes:

$$
\begin{aligned}
C_L &= C_{L\alpha}\left(\alpha+\frac{\dot{u}_z}{V}+(1-\bar{a})\frac{b\dot{\alpha}}{V}\right)\\
C_{M,E} &= C_{L\alpha}(\frac{1}{4}+\frac{1}{2}\bar{a})\left(\alpha+\frac{\dot{u}_z}{V}\right)+C_{L\alpha}(\frac{1}{4}\bar{a}-\frac{1}{2}\bar{a}^2)\frac{b\dot{\alpha}}{V}
\end{aligned}
\tag{12}
$$

where, the airfoil data has been replaced by the actual ones.

The physical meaning of the above equations are the lift of wing section is produced by steady and quasi-steady flow together, and the steady part is produced by the angle of attack α of the section and its increment $\dot{u}_z/V_0$ caused by relative elastic deformation. The quasi-steady part is caused by $\dot{\alpha}$.

It should be noted that, in most cases, the angles of attack in every sections (denoted as α_B) are not easy to be measured directly. Hence, the relationship between α_B and incident angle at the CG of UAV expressed in a_M-frame (notated as α_M and β_M) can be calculated as:

$$
\begin{aligned}
&-\sin\alpha_B = C_{a_B B}(3,1)\\
&=[0,0,1]C_{a_B a_M}C_{a_M M}C_{MB}[1,0,0]^T\\
&=(\cos\alpha_M\sin\beta_M\sin\varphi_{BM,x}-\sin\alpha_M\cos\varphi_{BM,x})\\
&*(\cos\varphi_{BM,y}\cos\varphi_{BM,z})\\
&+(\cos\beta_M\sin\varphi_{BM,x})(\cos\varphi_{BM,y}\sin\varphi_{BM,z})\\
&-(\sin\alpha_M\sin\beta_M\sin\varphi_{BM,x}+\cos\alpha_M\cos\varphi_{BM,x})\sin\varphi_{BM,y}
\end{aligned}
\tag{13}
$$

where, φ_{BM} is the Euler angle from B-frame to M-frame.

If the wing rotates along the x axis only, Eq. (13) can be simplified as:

$$\sin\alpha_B=-\cos\alpha_M\sin\beta_M\sin\varphi_{BM,x}+\sin\alpha_M\cos\varphi_{BM,x} \tag{14}$$

The magnitude of drag is small, and its influence on the flight dynamics characteristics is limited, so the drag on every wing section can be divided from the total drag averagely. The expression of total drag is:

$$C_D=C_{D0}+a_{induce}C_L^2 \tag{15}$$

The aerodynamics force expressed in a_M-frame can be derived by the following axis conversion:

$$\{f_a\}_{a_M}=C_{a_M a_B}\{f_a\}_{a_B} \tag{16}$$

where:

$$C_{a_M a_B}=\begin{bmatrix}1 & 0 & 0\\ 0 & \cos\varphi_{BM,x} & -\sin\varphi_{BM,x}\\ 0 & \sin\varphi_{BM,x} & \cos\varphi_{BM,x}\end{bmatrix} \tag{17}$$

Substituting Eq. (17) for Eq. (16)， the non-dimensional force coefficients at the a_M-coordinate are derived as follows：

$$
\begin{aligned}
\{C_D\}_{a_M} &= \{C_D\}_{a_B}\\
\{C_C\}_{a_M} &= \{C_L\}_{a_B}\sin\varphi_{BM,x}\\
\{C_L\}_{a_M} &= \{C_L\}_{a_B}\cos\varphi_{BM,x}
\end{aligned}
\tag{18}
$$

Change the reference point of moment into CG, the aerodynamics moment to CG of UAV is:

$$\{m_a\}_M = \{m_{a,0}\}_M + \{r\}_M \times (C_{Ma_M}\{f_a\}_{a_M}) \tag{19}$$

It should be noted that, the method proposed in this section can be used to calculate either the aerodynamics force or the moment of vertical tails, although the incident angle and Euler angle vary significantly.

3.3 3D effect correction of aerodynamics

In the analysis of the aeroelastic flight dynamics of solar-powered UAV, most papers ignored the aerodynamics force distribution characteristics along the wing span and considered the flow condition as the same as the airfoils. Actually, the wing span is finite, which will make the flow of each section affects each other, that is to say, 3D effect must be considered for precision. In this paper, 3D effect is corrected based on lifting-line theory, and it applies well to wings that have aspect ratio greater than 5 and sweep angle less than 20 degrees.

According to lifting-line theory, the lift of airfoil is determined by effective angle of attack α_{eff}, which is formulated as follows:

$$\alpha_{eff} = \alpha_{geo} - \alpha_{ind} \tag{20}$$

where, α_{geo} and α_{ind} represent geometric and induced angle of attack respectively.

According to the relationship of trailing vortex and circulation, the equation above becomes:

$$\alpha_{geo}(y_0) = \frac{\Gamma(y_0)}{\pi V_\infty c(y_0)} + \alpha_{L=0} + \frac{1}{4\pi V_\infty}\int_0^l \frac{(d\Gamma/dy)dy}{y_0 - y} \tag{21}$$

where, y_0 is an arbitrary spanwise position on the wing. 2π refers to theoretical lift slope of airfoil, which can be substituted by true airfoil value in the actual computation. Since Eq. (21) is a nonlinear integral-differential equation, coordinate transformation method should be applied before solving it for simplification [7].

After solving the circulation distribution $\Gamma(y)$ from Eq.(21)，the lift distribution can be obtained from the Kutta-Joukowski theorem:

$$L(y_0) = \rho V_\infty \Gamma(y_0) \tag{22}$$

By repeating the above steps for different geometric angles of attack and take a derivative, one can obtain the lift slope of each cross section of the wing considering 3D effect correction.

4 Linearized model

4.1 Linearized longitudinal aerodynamics

The movement of wing section is separated into two parts: the rigid movement of UAV and the elastic movement of structure. Then, the lift coefficients applied on the wing section can be deployed in the a_B-frame as follows:

$$\begin{aligned}
C_{L\alpha} &= C_{L\alpha}\\
C_{Lq} &= 0.5C_{L\alpha} + 2C_{L\alpha}\left(\frac{3}{4} - \{\bar{x}_g\}_s\right)\\
C_{Lp} &= -2C_{L\alpha}\frac{\{y_g\}_s}{l}\\
C_{L\varphi_y} &= C_{L\alpha}\\
C_{L\dot{u}_z} &= C_{L\alpha}\frac{1}{V}\\
C_{L\dot{\varphi}_y} &= C_{L\alpha}(1-\bar{a})\frac{c}{2V}
\end{aligned} \tag{23}$$

It should be noted that, the variables in the above equations are measured in the a_B-frame and B-frame.

According to the 2nd equation of Eq.(12), the aerodynamics moment to the elastic center (EC) is:

$$\begin{aligned}
C_{m\alpha,E} &= -C_{L\alpha}\{\bar{x}_{AE}\}_B \approx C_{L\alpha}\left(\frac{1}{4} + \frac{1}{2}\bar{a}\right)\\
C_{mq,E} &= 0.5C_{L\alpha}\{\bar{x}_{CE}\}_B + 2C_{L\alpha}\{\bar{x}_{Cg}\}_s\{\bar{x}_{AE}\}_B\\
C_{mp,E} &= -2C_{L\alpha}\frac{\{y_g\}_s}{l}\{\bar{x}_{AE}\}_B\\
C_{m\varphi_y,E} &= C_{m\alpha,E}\\
C_{m\dot{u}_z,E} &= C_{m\alpha,E}\frac{1}{V}\\
C_{m\dot{\varphi}_y,E} &= C_{L\alpha}\left(\frac{1}{4}\bar{a} - \frac{1}{2}\bar{a}^2\right)\frac{c}{2V}
\end{aligned} \tag{24}$$

From the 2nd equation of Eq.(18), the difference of lift expressed in the a_M-frame and a_B-frame are only $\cos\varphi_{BM,x}$. Hence, replace $C_{L\alpha}$ in Eq. (23) into $C_{L\alpha}\cos\varphi_{BM,x}$, the lift expressed in the a_B-frame will be derived.

Substituting the expression of lift at a_M-frame into Eq.(19), the pitch moment for the center of gravity of the UAV can be obtained as follows:

$$
\begin{aligned}
&C_{m\alpha,g}=-C_{L\alpha}\cos\varphi_{MB,x}(\{\bar{x}_A\}_s-\{\bar{x}_g\}_s)\\
&C_{mq,g}=C_{L\alpha}\cos\varphi_{MB,x}(0.5\{\bar{x}_{Cg}\}_B-2\{\bar{x}_{Cg}\}_B^{\ 2})\\
&C_{mp,g}=-2C_{L\alpha}\frac{\{y_g\}_s}{l}\{\bar{x}_{Cg}\}_B\\
&C_{m\varphi_y,g}=C_{m\alpha,g}\\
&C_{m\dot{u}_z,g}=C_{m\alpha,g}\frac{1}{V}\\
&C_{m\dot{\varphi}_y,g}=-2C_{L\alpha}\cos\varphi_{MB,x}(\frac{1}{2}-\{\bar{x}_g\}_s)^2\frac{b}{V}
\end{aligned}
\tag{25}
$$

4.2 linearized lateral-directional aerodynamics

In order to analyze the flight dynamics characteristic of lat-dir, the aerodynamics force derivatives should also be derived.

According to Eq.(14), the derivative of angle of attack to the side slip angle in a_B-frame is:

$$\partial\alpha_B/\partial\beta_M\approx-\sin\varphi_{BM,x}\cos\alpha_M\cos\beta_M \tag{26}$$

As in small disturbance equation the angle of side slip β_M usually is zero, the derivative of lift coefficient to β_M of wing section in a_B-frame can be calculated as follows:

$$C_{L\beta}=C_{L\alpha}\partial\alpha_B/\partial\beta_M\approx-C_{L\alpha}\cos\alpha_M\sin\varphi_{BM,x} \tag{27}$$

The derivative of lift coefficient to yaw rate can be derived as follows:

$$C_{Lr}=2C_L\frac{\{y_g\}_s}{l} \tag{28}$$

According to Eq. (27) and (28), and with the expressions of side force coefficient C_y, roll moment C_l and yaw moment C_n and the assumption that the wing rotates along the x axis only, the side force coefficient derivatives can be derived as follows:

$$
\begin{aligned}
&C_{y\beta}=-C_D-C_{L\alpha}\sin^2\varphi_{BM,x}\\
&C_{yp}=2C_{L\alpha}\sin\varphi_{BM,x}(\{y_g\}_s/l)\\
&C_{yr}=-2C_L\sin\varphi_{BM,x}(\{y_g\}_s/l)\\
&C_{y\dot{u}_z}=C_{L\dot{u}_z}\sin\varphi_{BM,x}\\
&C_{y\dot{\varphi}_y}=C_{L\dot{\varphi}_y}\sin\varphi_{BM,x}\\
&C_{y\varphi_y}=C_{L\varphi_y}\sin\varphi_{BM,x}
\end{aligned}
\tag{29}
$$

Roll moment coefficient derivatives are:

$$
\begin{aligned}
&C_{l\beta}=0.5C_{L\alpha}\sin(2\varphi_{BM,x})\cos^2\alpha\{y_g\}_s/l\\
&C_{lp}=-2C_{L\alpha}\cos\varphi_{BM,x}\cos\alpha(\{y_g\}_s/l)^2\\
&C_{lr}=2C_L(\cos\varphi_{BM,x}\cos\alpha+\sin\varphi_{BM,x})(\{y_g\}_s/l)^2\\
&C_{l\dot{u}_z}=-C_{L\dot{u}_z}\cos\varphi_{BM,x}\cos\alpha\{y_g\}_s/l\\
&C_{l\dot{\varphi}_y}=-C_{L\dot{\varphi}_y}\cos\varphi_{BM,x}\cos\alpha\{y_g\}_s/l\\
&C_{l\varphi_y}=-C_{L\varphi_y}\cos\varphi_{BM,x}\cos\alpha\{y_g\}_s/l
\end{aligned}
\tag{30}
$$

Yaw moment coefficient derivatives are:

$$
\begin{aligned}
&C_{n\beta}=(C_L\cos\alpha-C_{L\alpha}\alpha)\varphi_{BM,x}\{y_g\}_s/l\\
&C_{np}=-2C_{L\alpha}\cos\varphi_{BM,x}\sin\alpha(\{y_g\}_s/l)^2\\
&C_{nr}=2C_L\cos\varphi_{BM,x}\sin\alpha(\{y_g\}_s/l)^2\\
&C_{n\dot{u}_z}=-C_{L\dot{u}_z}\cos\varphi_{BM,x}\sin\alpha\{y_g\}_s/l\\
&C_{n\dot{\varphi}_y}=-C_{L\dot{\varphi}_y}\cos\varphi_{BM,x}\sin\alpha\{y_g\}_s/l\\
&C_{n\varphi_y}=-C_{L\varphi_y}\cos\varphi_{BM,x}\sin\alpha\{y_g\}_s/l
\end{aligned}
\tag{31}
$$

4.3 Linearized flight dynamics equation

It can be found that the form of Eq. (4) and (5) is the same as that of flight dynamics equations of normal rigid vehicles. Hence, they can be linearized by small disturbance method too, and written into two sets of equations: longitudinal and lateral-directional. Different from the normal rigid vehicle, the external force such as aerodynamics, thrust and gravity are related to rigid motion and elastic motion for elastic model. The linear equation of flight dynamics for elastic UAV is:

$$\dot{\boldsymbol{x}}_r=\boldsymbol{A}_r\boldsymbol{x}_r+\boldsymbol{B}_r\boldsymbol{u}_r+\boldsymbol{A}_{re}\boldsymbol{x}_e \tag{32}$$

where, $\boldsymbol{A}_r$ and $\boldsymbol{B}_r$ is the same as conventional rigid vehicles as shown in Ref. [8]; $\boldsymbol{x}_r$ is the independent variable of rigid motion, with $\boldsymbol{x}_r=[v,\alpha,q,\theta]^T$ in longitudinal equations and $\boldsymbol{x}_r=[\beta,p,r,\phi]^T$ in lat-dir equations; $\boldsymbol{x}_e=[\dot{u}_z{}^T,\dot{\varphi}_y{}^T,u_z{}^T,\varphi_y{}^T]^T$ is the independent variable of elastic motion; $\boldsymbol{A}_{re}$ is the influence matrix of elastic motion to rigid motion, for longitudinal:

$$
\boldsymbol{A}_{re}=\begin{bmatrix}
0_{1\times n} & 0_{1\times n} & 0_{1\times n} & 0_{1\times n}\\
Z_{\dot{u}_z,1}\cdots Z_{\dot{u}_z,n} & Z_{\dot{\varphi}_y,1}\cdots Z_{\dot{\varphi}_y,n} & 0_{1\times n} & Z_{\varphi_y,1}\cdots Z_{\varphi_y,n}\\
M_{\dot{u}_z,1}\cdots M_{\dot{u}_z,n} & M_{\dot{\varphi}_y,1}\cdots M_{\dot{\varphi}_y,n} & 0_{1\times n} & M_{\varphi_y,1}\cdots M_{\varphi_y,n}\\
0_{1\times n} & 0_{1\times n} & 0_{1\times n} & 0_{1\times n}
\end{bmatrix}
$$

and for lat-dir is:

$$\boldsymbol{A}_{re}=\begin{bmatrix} Y_{\dot{u}_z,1}\cdots Y_{\dot{u}_z,n} & Y_{\dot{\varphi}_y,1}\cdots Y_{\dot{\varphi}_y,n} & 0_{1\times n} & Y_{\varphi_y,1}\cdots Y_{\varphi_y,n} \\ L_{\dot{u}_z,1}\cdots L_{\dot{u}_z,n} & L_{\dot{\varphi}_y,1}\cdots L_{\dot{\varphi}_y,n} & 0_{1\times n} & L_{\varphi_y,1}\cdots L_{\varphi_y,n} \\ N_{\dot{u}_z,1}\cdots N_{\dot{u}_z,n} & N_{\dot{\varphi}_y,1}\cdots N_{\dot{\varphi}_y,n} & 0_{1\times n} & N_{\varphi_y,1}\cdots N_{\varphi_y,n} \\ 0_{1\times n} & 0_{1\times n} & 0_{1\times n} & 0_{1\times n} \end{bmatrix}$$

The details of $\boldsymbol{A}_{re}$ can be seen in ref. [9].

4.4 Linearized structure dynamics equation

Ignoring non-linear coupling terms in Eq. (1), and assuming that the translational strain is small and the external moment and the moment of inertia of x and z direction are equal to zero, Eq. (1) can be reduced into:

$$\begin{aligned} &\mu\dot{V}_x = EI_z\kappa_z'' + f_x \\ &\mu\dot{V}_z = -EI_x\kappa_x'' + f_z \\ &I_{yy}\dot{\Omega}_y = EI_y\kappa_y' + m_z \\ &\dot{\kappa}_x = V_z'' \\ &\dot{\kappa}_y = \Omega_y' \\ &\dot{\kappa}_z = -V_x' \\ &\mu\dot{V}_y = f_y \end{aligned} \tag{33}$$

The equations above can be rearranged into a compact form as follows:

$$\begin{aligned} &\mu\ddot{x} + EI_z x'''' = f_x \\ &\mu\ddot{z} + EI_x z'''' = f_z \\ &I_{yy}\ddot{\varphi}_{Bg,y} - GJ_z\varphi_{Bg,y}'' = m_y \\ &\mu\dot{V}_y = f_y \end{aligned} \tag{34}$$

Since the focus of this paper is the flight dynamics characteristics of the total UAV, the structure dynamics characteristics is used to derive the increase of aerodynamics force caused by aeroelastic only and many assumptions for simplification can be introduced to linearize the equations above.

Eq. (34)can be simplified to the form as in Eq. (35)by rewriting in *M*-frame and assuming that the structure elastic vibrancy is limited in a little area near the balanced states and the elastic motion in *x* direction is ignorable. In the case of geometry, it is assumed that the *M*-frame is parallel to *R*-frame and the sweep angle of wing is zero. Besides, in mean axis system, the elastic motion is influenced by rigid motion through aerodynamics force only.

$$\begin{aligned} &\mu\{\ddot{u}_z\}_{M,z} + EI_x\{u_z\}_{M,z}'''' = \cos\varphi_{BM,x}\{f\}_{B,z} \\ &I_{yy}\ddot{\varphi}_{BM,y} - GJ_z\varphi_{BM,y}'' = \{m\}_{B,y} \end{aligned} \tag{35}$$

where, $\varphi_{BM,y}$ represents the angle between x axis of *B*-frame and the *oxy* plane of *M*-frame. All variables in Eq. (35)are in incremental form and the notation Δ has been neglected for simplification.

Replacing the spatial derivatives by Eq. (3), and knowing the fact that the wing tip is free, the boundary conditions can be defined that the bending moments and shear forces at the first and last nodes are zero for the 1st equation in Eq. (35), that is [3]:

$$\begin{aligned} &u_{z,1}'' = 0, u_{z,n}'' = 0 \\ &u_{z,1}''' = 0, u_{z,n}''' = 0 \end{aligned} \tag{36}$$

Thus the structure dynamics equation can be derived as follows:

$$M_{u_z}\ddot{u}_z + K_{u_z}u_z = Q_{u_z} \tag{37}$$

where:

$$u_z = [u_1 \;\cdots\; u_n]^T$$

$$M_{u_z} = \begin{bmatrix} \mu_1 & & \\ & \ddots & \\ & & \mu_n \end{bmatrix}$$

$$K_{u_z} = \begin{bmatrix} 2 & -4 & 2 & & & & \\ -2 & 5 & -4 & 1 & & & \\ 1 & -4 & 6 & -4 & 1 & & \\ & \ddots & \ddots & \ddots & \ddots & \ddots & \\ & & 1 & -4 & 6 & -4 & 1 \\ & & & 1 & -4 & 5 & -2 \\ & & & & 2 & -4 & 2 \end{bmatrix} * \frac{1}{\Delta l^4} diag(EI_{z,i})$$

For the 2nd equation in Eq.(35), the boundary conditions are [3]:

$$\varphi_{BM,y,1}' = 0, \varphi_{BM,y,n}' = 0 \tag{38}$$

Then the structure dynamics equation becomes:

$$M_{\varphi_y}\ddot{\varphi}_y + K_{\varphi_y}\varphi_y = Q_{\varphi_y} \tag{39}$$

where:

$$\varphi_y = \left[\varphi_{BM,y,1} \ \cdots \ \varphi_{BM,y,n}\right]^T$$

$$M_{\varphi_y} = \begin{bmatrix} I_1 & & \\ & \ddots & \\ & & I_n \end{bmatrix}$$

$$K_{\varphi_y} = -\begin{bmatrix} -2 & 2 & & & \\ 1 & -2 & 1 & & \\ & \ddots & \ddots & \ddots & \\ & & 1 & -2 & 1 \\ & & & 2 & -2 \end{bmatrix} * \frac{1}{\Delta l^2} diag(GJ_i)$$

In order to further simplify the linear structure dynamics equations, Eq. (37) and (39) can be expanded in the modal coordinate system, and the final form can be derived as follows:

$$\dot{\boldsymbol{x}}_{ne} = \boldsymbol{A}_{ne}\boldsymbol{x}_{ne} + \boldsymbol{A}_{ner}\boldsymbol{x}_r \tag{40}$$

where, the independent variables are:

$$\boldsymbol{x}_{ne} = \begin{bmatrix} \dot{\boldsymbol{x}}_n \\ \boldsymbol{x}_n \end{bmatrix}, \ \boldsymbol{x}_e = \mu \boldsymbol{x}_n, \ \boldsymbol{x}_e = [u_z^T, \varphi_y^T]^T$$

where, $\boldsymbol{x}_n$ is the modal of structure elastic motion, which is the symmetric modes for longitudinal motion and asymmetric modes for lat-dir motion; μ is the transfer matrix from modal frame to physical frame.

For longitudinal motion, the coefficient matrices in Eq. (40) are:

$$A_{ne} = \begin{bmatrix} M_n^{-1}Q_{n1} & M_n^{-1}(Q_{n2} - K_n) \\ I & 0 \end{bmatrix}, \ A_{ner} = \begin{bmatrix} Q_{n0} \\ 0 \end{bmatrix},$$

$$M_n = \mu^T M \mu 、 K_n = \mu^T K \mu 、 Q_n = \mu^T Q$$

$$Q_{n0} = \mu^T Q_0$$

$$Q_{n1} = \mu^T Q_1 \mu$$

$$Q_{n2} = \mu^T Q_2 \mu$$

$$Q_0 = \begin{bmatrix} Z_{v,1} & Z_{\alpha,1} & Z_{q,1} & \\ \vdots & \vdots & \vdots & 0_{n\times1} \\ Z_{v,n} & Z_{\alpha,n} & Z_{q,n} & \\ M_{v,1} & M_{\alpha,1} & M_{q,1} & \\ \vdots & \vdots & \vdots & 0_{n\times1} \\ M_{v,n} & M_{\alpha,n} & M_{q,n} & \end{bmatrix}$$

$$Q_1 = \begin{bmatrix} Z_{\dot{u}_z,1} \cdots Z_{\dot{u}_z,n} & Z_{\dot{\varphi}_y,1} \cdots Z_{\dot{\varphi}_y,n} \\ M_{\dot{u}_z,1} \cdots M_{\dot{u}_z,n} & M_{\dot{\varphi}_y,1} \cdots M_{\dot{\varphi}_y,n} \end{bmatrix}$$

$$Q_2 = \begin{bmatrix} 0_{1\times n} & Z_{\varphi_y,1} \cdots Z_{\varphi_y,n} \\ 0_{1\times n} & M_{\varphi_y,1} \cdots M_{\varphi_y,n} \end{bmatrix}$$

where, $Z_{\dot{u}_z}$ is related to some derivatives (e.g. $C_{L\dot{u}_z}$). The exact expressions are the same as the derivatives of general flight dynamics equations. More details about them can be referred to Ref. [9].

For lat-dir motion, the coefficient matrix in Eq. (40) is:

$$Q_0 = \begin{bmatrix} Z_{\beta,1} & Z_{p,1} & Z_{r,1} & \\ \vdots & \vdots & \vdots & 0_{n\times1} \\ Z_{\beta,n} & Z_{p,n} & Z_{r,n} & \\ M_{\beta,1} & M_{p,1} & M_{r,1} & \\ \vdots & \vdots & \vdots & 0_{n\times1} \\ M_{\beta,n} & M_{p,n} & M_{r,n} & \end{bmatrix}$$

The expressions of other coefficient matrices are similar to longitudinal ones, but the modal x_n and transfer matrix μ are different.

4.5 Total linearized equation

Combined with Eq. (32) and(40), the final total linear equations can be derived as follows:

$$\begin{aligned} \dot{\boldsymbol{x}}_r &= \boldsymbol{A}_r\boldsymbol{x}_r + \boldsymbol{B}_r\boldsymbol{u}_r + \boldsymbol{A}_{rne}\boldsymbol{x}_{ne} \\ \dot{\boldsymbol{x}}_{ne} &= \boldsymbol{A}_{ner}\boldsymbol{x}_r + \boldsymbol{A}_{ne}\boldsymbol{x}_{ne} \end{aligned} \tag{41}$$

the independent variable is:

$$\boldsymbol{x} = [\boldsymbol{x}_r^T, \boldsymbol{x}_{ne}^T]^T \tag{42}$$

and the state matrix is:

$$A = \begin{bmatrix} A_r & A_{rne} \\ A_{ner} & A_{ne} \end{bmatrix} \tag{43}$$

The eigenvalues of the above state matrix are the modal eigenvalues of the elastic UAV considering the coupling of aeroelastic and flight dynamics.

5 Trimming

Aerodynamics model is the most complex and important external force model in the problem of flight dynamics, so it must be check carefully before numerical computation. The lift coefficient distribution along the wing span obtained from two methods are compared in Fig.3, one is derived from the Thin-Strip lifting-line theory proposed in section 3.3 in this paper, the other is the Vortex-Lattice method from AVL. It can be seen that the precision of Thin-Strip lifting-line theory model can satisfy the application requirements of this paper.

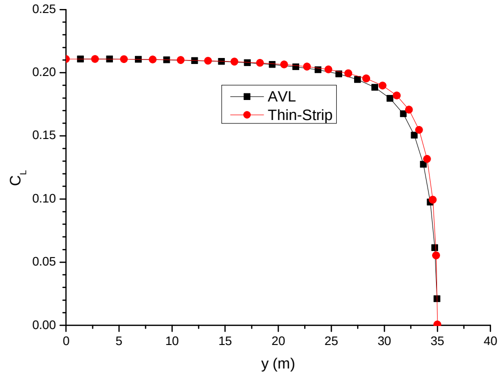

Fig.3 comparison of lift coefficient distribution along the spanwise

Four kinetics and aerodynamics models are selected and combined for comparison. Three kinetics models are employed: the "Undeformed" model represents the common rigid flight dynamics model; the "linear" model is that, the structure deformation is calculated from Eq.(37) and(39), while the equation of motion of UAV is descript by Eq.(4) and(5), this model is the same as provided in ref.[10]; the "nonlinear" model corresponds to Eq.(1). Two steady aerodynamics models are employed: one is the "2D aerodynamics" model, in which aerodynamics force at every wing section is regarded as the same as the airfoil, the other is the "3D aerodynamics", in which the Thin-Strip lifting-line theory model is employed to calculate the lift and drag distribution at the wing.

In level flight, the flapwise position and pitch angle of UAV are shown in Fig.4 and Fig.5. The trimming parameters are shown in Table 2.

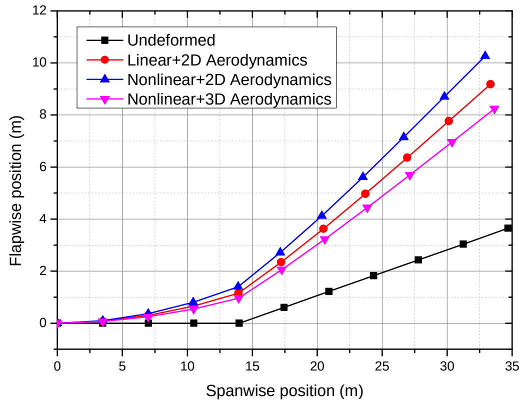

Fig.4 Flapwise position of UAV of different calculation model

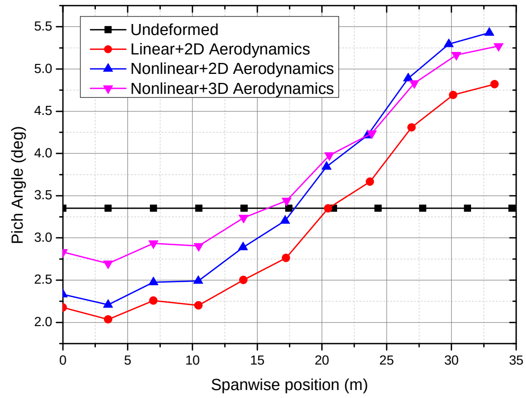

Fig.5 Pitch angle of UAV of different calculation model

Table 2 Trimming parameters of the UAV of different calculation model

	AOA at wing root (deg)	δ_e (deg)	δ_t
Undeformed	3.3502	0.5136	0.2318
Linear+2D Aerodynamics	2.1757	0.6401	0.1710
Nonlinear +2D Aerodynamics	2.3318	0.3311	0.2774
Nonlinear +3D Aerodynamics	2.8326	0.1408	0.2511

It can be concluded that the nonlinear+3D aerodynamics model's maximum wing deformation is 13%. By contrast, when applying the nonlinear+2D aerodynamics model which excludes the 3D effect, the aerodynamic force near the wingtip is larger than the actual one, leading to the deformation up to 19%. As for linear+2D aerodynamics model, since geometrically nonlinear effect is not considered, the pitch angle distribution is about 0.6 deg smaller, which will influence the UAV's drag and thrust direction, enlarge the difference of the magnitude of throttle control (δ_t) and bring fatal error to estimate the endurance of solar-powered UAV.

6 Modal analysis

The "Underformed" and "Deformed" models are corresponding to conventional rigid vehicles, and the linear "Flexible" model is based on Eq.(41). The longitudinal and latitudinal modes of different calculation models are shown in Table 3 and Table 4.

Table 3 Roots of Longitudinal mode of Different Calculation Models

	Short Period	Phugoid	1st bending
Undeformed	-6.710±3.925i	-0.046±1.003i	/

Deformed	-5.985±3.100i	-0.002±1.063i	/
Flexible	-0.394±1.707i	0.002±1.031i	-3.819±1.459i

Table 4 Roots of Latitudinal mode of Different Calculation Models

	Dutch	Roll	Spiral
Undeformed	-0.3615±0.5913i	-23.0637	-0.0277
Deformed	-0.3314±1.0335i	-22.8121	-0.0873
Flexible	-0.354±1.048i	-22.836	-0.094

The results showed that, the difference of three models is huge in longitudinal mode. Since the deformation of wing has increased the UAV's moment of inertia about the pitch axis, the frequency of short period mode has obviously decreased for the deformed model. The serious coupling between short period mode and 1st bending mode also significantly influences the roots of short period mode, which then results in the phugoid changing from stable to unstable. Through these analyses, it is clear that the flexible model is the only one which is able to accurately estimate the longitudinal flight dynamics behaviors.

As to lat-dir mode, considering the influence of deformation, the equivalent increase of dihedral angle leads to the increase *of* $C_{l\beta}$ and larger frequency of Dutch. The main difference between deformed model and flexible model is introduced by anti-symmetric deformation modes of wing. Since they have less influence on lat-dir aerodynamics force, the deformed model is quite accurate for lat-dir flight dynamics analysis.

7 Conclusions

In this paper, a geometrically nonlinear intrinsic beam model is introduced to establish the equation of motion of flexible solar-powered UAV, based on it, the decoupled linear flight dynamics and structure dynamics equations of motions are derived in mean axis frame.

Steady aerodynamics model is derived by theoretical airfoil data and corrected for 3D effect by lifting-line theory, quasi-steady aerodynamics model is derived by Theodorsen unsteady aerodynamics model, the aerodynamics derivatives of every wing sections are derived and transfer to different frames for the multi-role in linear equations of flight dynamics or structure dynamics.

The nonlinear+3D aerodynamics model's maximum wing deformation is 13%. By contrast, the nonlinear+2D aerodynamics model led to the deformation up to 19%, which is because the aerodynamic force near the wingtip is larger than actual ones. As for linear+2D aerodynamics model, since geometrically nonlinear effect is not considered, the pitch angle distribution is about 0.6 deg smaller, which will influence the UAV's drag and thrust direction, and bring fatal error to estimate the endurance of solar-powered UAV.

The results of modal analysis show that, the flexible model is the only one which is able to accurately estimate the longitudinal flight dynamics behaviors. The deformed model is quite accurate for lat-dir flight dynamics analysis.

8 Acknowledgments

This work is supported by the National Natural Science Foundation of China (11202162). The authors gratefully acknowledge the valuable advices from Professor Wang Zhengping and Doctor Wang Wei from the school of aeronautics, Northwestern Polytechnical University.

References

[1] Dewey H. Hodges. A Mixed Variational Formulation Based on Exact Intrinsic Equation for Dynamics of Moving Beams. *International Journal of Solids and Structures*. Vol. 26, No. 11, pp 1253 -1273, 1990.

[2] Mayuresh J. Patil, Dewey H. Hodges. Flight dynamics of highly flexible flying wings. *Journal of Aircraft*. Vol. 43, No. 6, pp 1790-1798, 2006.

[3] Rafael Palacios, Joseba Murua, Robert Cook. Structural Aerodynamic Models in Nonlinear Flight Dynamics of Very flexible Aircraft. *AIAA Journal*, Vol. 48, No. 11, pp 2648-2659, 2010.

[4] Singiresu S, Rao. *Mechanical vibrations*. 4th edition, Pearson Education Inc, United States of America. 2004.

[5] Brijesh Raghavan. *Flight Dynamics and control of highly flexible flying-wing*. PH.D. thesis, Virginia Polytechnic Institute and State University, 2009.

[6] Hodges, D. H. Geometrically exact, intrinsic theory for dynamics of curved and twisted anisotropic beams. *AIAA Journal*. Vol. 41, No. 6, pp 1131-1137, 2003.

[7] Anderson, J. D. Fundamentals of Aerodynamics. 4th edit, McGraw-hill Companies, Inc, 2007.
[8] Fang Zhenping, Chen Wanchun, Zhang Shuguang. *Aeronautic vehicle flight dynamics.* 1st edition, Beihang University Press, 2005. (in chinease)
[9] Wang Rui. *Research on dynamics and control of highly flexible solar-powered UAV*. Postdoctoral report, Northwestern Polytechnology University, xi'an, China. (in chinease)
[10] Martin R. Waszak, David K, Schmidt. Flight dynamics of aeroelastic vehicle. *Journal of Aircraft*, Vol 25, No. 6, pp 563-571, 1988.

8.1 Copyright statement